An Adaptive Particle Filtering-based Framework for Real-time Fault Diagnosis and Failure Prognosis of Environmental Control Systems

Ioannis A. Raptis [1], George Vachtsevanos [1]

[1] *Department of Electrical and Computer Engineering, Georgia Institute of Technology, Atlanta, GA, 30332, USA.*
iraptis@gatech.edu
gjv@ece.gatech.edu

ABSTRACT

Maintenance of critical or/complex systems has recently moved from traditional preventive maintenance to Condition Based Maintenance (CBM) exploiting the advances both in hardware (sensors / DAQ cards, etc.) and in software (sophisticated algorithms blending together the state of the art in signal processing and pattern analysis). Along this path, Environmental Control Systems and other critical systems/processes can be improved based on concepts of anomaly detection, fault diagnosis and failure prognosis. The enabling technologies borrow from the fields of modeling, data processing, Bayesian estimation theory and in particular a technique called particle filtering. The efficiency of the diagnostic approach is demonstrated via simulation results.

1. INTRODUCTION

Heating, Ventilating and Air Conditioning (HVAC) systems have a large span of applications ranging from industrial buildings, households to small scale units installed in aerial and ground vehicles operating as part of Environmental Control Systems (ECS). Defective or faulty operation of such systems have both environmental and economical impact. Typical drawbacks are high operating cost, maintenance cost and thermal discomfort.

A standard ECS system is composed of four main components that are encountered in subcritical vapor compression cycles: The evaporator, condenser, Thermostatic Expansion Valve (TEV) and compressor. The refrigerant enters the compressor as a superheated vapor at a low pressure. In the compressor, the refrigerant is compressed to a high pressure and it is routed to the condenser. At this higher pressure, the refrigerant has a higher temperature than the ambient conditions and the refrigerant condenses. The refrigerant exits the condenser as a subcooled liquid at a higher pressure and passes through the thermostatic expansion device. At the exit of the expansion valve, the refrigerant is at low pressure and routed to the evaporator. At this lower pressure the refrigerant has a lower temperature than ambient conditions, therefore heat is transferred to the refrigerant, and the refrigerant evaporates. Finally the refrigerant re-enters the compressor and the cycle is repeated. The main components as well as the several phases of the thermo-fluid in a vapor compression cycle with two-phase heat exchangers are depicted in Figure 1.

From first principles modeling, the dynamic behavior of thermo-fluid systems is dictated by highly coupled, nonlinear partial differential equations. Such equations are both complicated to handle for analysis and conducting numerical simulations. The main difficulty in the dynamic modeling of vapor compression cycles is the representation of the thermo-fluid inside the two-phase heat exchanger. Wedekind's work (Wedekind, Bhatt, & Beck, 1978) indicated that two-phase transient flow problems can be converted into lumped-parameter systems of nonlinear ordinary differential equations assuming that the mean void fraction remains relatively invariant in the two-phase section of a heat exchanger. This approach has also been adopted in this paper following the work reported in (X. He, 1996; X.-D. He & Asada, 2003; Rasmussen, 2005).

The ECS systems are subjected to various fault conditions. A survey for the most common faults encountered in ECS systems is given in (Comstock, Braun, & Groll, 2002). In this paper, the fault under consideration is the refrigerant leakage that takes place in the evaporator. According to (Braun, 2003), refrigerant leakage accounts for about 12% of the total service calls in response to a loss of cooling. All refrigeration systems have the potential to leak because pressures in the system are usually many times higher than atmospheric. Loss of refrigerant from industrial and commercial refrigeration systems can occur: (a) due to gradual leakage from joints or seals (b) through accidental rapture of a pipe or joint takes place and results in a significant loss of refrigerant charge in a short period of time and (c) during servicing when some refrigerant can be accidentally vented to gain access to a section of pipe or a given piece of equipment for repair.

A statistical rule-based method for Fault Detection

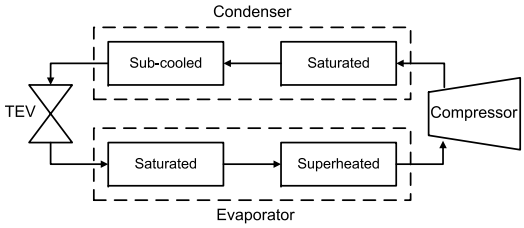

Figure 1: Main components of the vapor compression cycles and thermo-fluid phases

and Diagnosis (FDD) has been applied in for packaged air conditioning systems in (Li & Braun, 2003; Rossi & Braun, 1997) and for rooftop air conditioner in (Breuker & Braun, 1998). In (Stylianou & Nikanpour, 1996), an FDD method is employed for reciprocating chillers utilizing physical modeling, pattern recognition and expert knowledge. An on-line refrigerant leakage detection scheme is proposed in (Navarro-Esbri, Torrella, & Cabello, 2006) using adaptive algorithms.

This paper presents the implementation of an on-line particle-filtering-based framework for fault diagnosis and failure prognosis in a two-phase heat exchanger of an ECS. The methodology considers an autonomous module, and assumes the existence of fault indicators (for monitoring purposes) and the availability of real-time measurements. The fault detection and identification (FDI) module uses a hybrid state-space model of the plant, and a particle filtering algorithm to calculate the probability of leakage in the evaporator; simultaneously computing the state probability density function (pdf) estimates.

The failure prognosis module, on the other hand computes the remaining useful life (RUL) estimate of the faulty subsystem in real time, using the the detection algorithm current state estimates of the nonlinear state-space fault growth model and predicts the evolution in time of the probability distribution of the leaked mass.

The enabling technologies borrow from the fields of modeling, data processing, Bayesian estimation theory and in particular a technique called particle filtering. The proposed FDI framework is enhanced with an additional particle filtering routine that is executed in parallel with the state estimator, which estimates the unknown model parameters of the leakage progression model. The simulation result indicate that the proposed dual particle filtering scheme is highly adaptive and reliable even for abrupt crack that cause leakage.

This methodology allows the inclusion of customer specifications (statistical confidence in fault detection, minimum prediction window, etc.) in a simple and direct way. Moreover, all the outcomes are easily provided to plant operators through real-time updated graphs and may be easily coded and embedded in compact modules.

This paper is organized as follows: Section 2 presents the evaporator model which was used for the numerical simulations. In Section 3 the leakage flow rate progression model is given. The technical approach of the detection algorithm is presented in Section 4. The prognostic module is presented in Section 5. Results in the form of numerical simulations are given in Section 6. Finally, concluding remarks are given in Section 7.

2. EVAPORATOR MODELING

For the dynamic representation of the evaporator, this paper adopts the modeling approach introduced by (Grald & MacArthur, 1992; X.-D. He & Asada, 2003; Cheng, He, & Asada, 2004). This approach is based on the work reported in (Wedekind et al., 1978) where a mean void fraction is used in the two-phase region of the heat exchanger. The model converts the two-phase evaporating flow system into a type of lumped parameter system. The dynamics of the two heat exchangers use a moving boundary layer model to separate the distinct two-phase liquid from the single-phase superheated of the evaporator. Based on (X. He, 1996), the fundamental standing assumptions of the heat exchangers dynamic model are:

1. One dimensional fluid flow
2. Negligible heat conduction along the axial directions of heat exchangers
3. Invariant mean void fraction in the two-phase sections during a short transient
4. Negligible refrigerant pressure drop along the heat exchangers

Using the mean void fraction assumption the mass balance equation can be written as:

$$\frac{d}{dt}\left\{\left[\rho_l\left(1-\bar{\gamma}\right)+\rho_g\bar{\gamma}\right]A_t l_e\right\}=\dot{m}_{in}-\dot{m}_{mid} \quad (1)$$

where $\bar{\gamma}$ is the mean void fraction, l_e is the tube length that corresponds to the two-phase section, A_t is the cross section area of the tube, $\dot{m}_{in}$ is the inlet flow rate, $\dot{m}_{mid}$ is the flow rate of the moving boundary, and ρ_l, ρ_g are the refrigerant's liquid and vapor density in the two-phase section. The energy balance equation can be written as:

$$\frac{d}{dt}\left\{\left[\rho_l h_l\left(1-\bar{\gamma}\right)+\rho_g h_g\bar{\gamma}\right]A_t l_e\right\}= \underbrace{\left[h_l\left(1-x\right)+h_g x\right]}_{h_{in}}\dot{m}_{in}-h_g\dot{m}_{mid}+\underbrace{l_e\pi U_w D_t\left(T_w-T_e\right)}_{Q(l_e,T_e,T_w)} \quad (2)$$

where x is the inlet vapor quality, D_t is the diameter of the tube, U_w is the heat transfer coefficient between the tube wall and the refrigerant, T_e is the temperature of the refrigerant in the two-phase section, T_w is the temperature of the tube wall, and h_l, h_g are the specific enthalpies of the refrigerant liquid and vapor, respectively. The first term in the right hand side of Eq. (2) represents the rate at which energy enters the two-phase region by the inlet mass flow rate, the second term represents the rate at which thermal energy exits the two-phase region, by the outlet mass flow rate. The last term represent the heat transfer rate from the tube wall to the refrigerant. Multiplying Eq. (1) with h_g and subtracting Eq. (2) one gets:

$$\frac{d}{dt}\left[\rho_l\left(1-\bar{\gamma}\right)h_{lg}A_t l_e\right]=\left(1-x\right)h_{lg}\dot{m}_{in}-Q \quad (3)$$

where $h_{lg}=h_g-h_l$. Assuming that the refrigerant properties remain constant over the time step, the moving boundary dynamics can be written as:

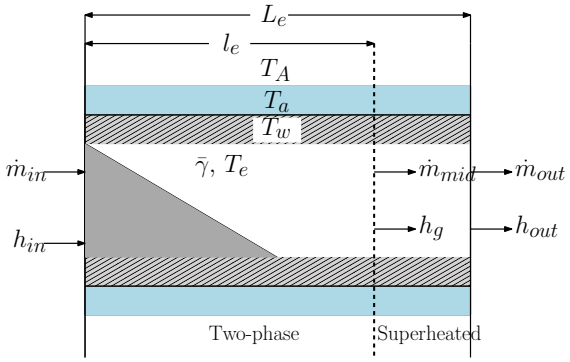

Figure 2: Schematic of the evaporator

$$\frac{dl_e}{dt} = -\frac{\pi U_w D_t \left(T_w - T_e\right)}{\rho_l \left(1-\bar{\gamma}\right) h_{lg} A_t} l_e + \frac{1-x}{\rho_l \left(1-\bar{\gamma}\right) A_t} \dot{m}_{in} \quad (4)$$

The dynamic equation of the system's second state variable is produced by the vapor balance in the evaporator. The vapor mass flow rate entering the evaporator is $\dot{m}_{in}x$. The vapor mass flow rate exiting the evaporator is $\dot{m}_{out}$ while the rate of vapor generated from liquid during the evaporation process in the two-phase section is $Q(l_e, T_e, T_w)/h_{lg}$. Assuming that in the evaporator the vapor volume is significantly larger than the liquid volume, the vapor balance equation is given by:

$$\frac{dm_e}{dt} = V_e \frac{d\rho_g}{dt} = \dot{m}_{in}x - \dot{m}_{out} + \frac{Q}{h_{lg}} \quad (5)$$

where m_e and V_e are the total vapor mass and total volume of the evaporator. Since ρ_g is the denotes the vapor saturated density, from the state equation one can easily obtain the one-to-one mapping $T_e\left(\rho_g(t)\right)$.

It is assumed that the wall temperature is spatially uniform. The one dimensional energy balance equation for the tube wall is given by

$$c_w p_w A_w \frac{dT_w}{dt} = U_w A_w (T_e - T_w) + U_a A_a (T_a - T_w) \quad (6)$$

where c_w, p_w and A_w are the specific heat, density and cross sectional area of the tube wall, respectively. In addition, U_a denotes the heat transfer coefficient between the tube wall and the air, $A_a$the surface area between the tube wall and the air and T_a the air exiting temperature from the evaporator. Similarly, assuming that the air exit temperature is spatially uniform, the one dimensional energy balance equation can be written as

$$c_a p_a A_a \frac{dT_a}{dt} = U_w A_w (T_w - T_a) + \dot{m}_a (T_A - T_a) \quad (7)$$

where c_a, p_a and A_a are the specific heat, density and cross sectional area of the air tube, respectively. The variable T_A denotes the air temperature at the entrance of the evaporator and $\dot{m}_a$ the air flow rate.

3. REFRIGERANT LEAKAGE MODEL

The refrigerant leakage is produced typically by a crack in the system pipes or by a faulty connection of the pipe system joints. Based on (Merritt, 1967), the mass flow rate of the leaked refrigerant is given by the following equation:

$$\frac{dm_{leak}}{dt} = c_d A_l \sqrt{2\rho(P - P_o)} \quad (8)$$

where m_{leak} is the mass of the leaked refrigerant, c_d is the discharge coefficient, A_l is the crack surface, ρ is the refrigerant density, P is the refrigerant pressure inside the pipe and P_o is the refrigerant pressure outside the pipe. Assuming that the outer pressure is significantly smaller than the refrigerant pressure inside the pipe, the refrigerant leakage growth model can be approximated by:

$$\frac{dm_{leak}}{dt} = C_r \sqrt{\rho_l P_e} \quad (9)$$

where P_e is the refrigerant pressure in the two-phase section of the evaporator $C_r = \sqrt{2} c_d A_l$.

4. TECHNICAL APPROACH - THE DIAGNOSTIC ALGORITHMS

A fault diagnosis procedure involves the tasks of fault detection and isolation (FDI), and fault identification (assessment of the severity of the fault). In general, this procedure may be interpreted as the fusion and utilization of the information present in a feature vector (measurements), with the objective of determining the operating condition (state) of a system and the causes for deviations from particularly desired behavioral patterns. Several ways to categorize FDI techniques can be found in literature. FDI techniques are classified according to the way that data is used to describe the behavior of the system: *data-driven* or *model-based* approaches.

Data-driven FDI techniques (Chen, Zhang, & Vachtsevanos, n.d.; Chen, Vachtsevanos, & Orchard, 2010) usually rely on signal processing and knowledge-based methodologies to extract the information hidden in the feature vector (also referred to as measurements). In this case, the classification/prediction procedure may be performed on the basis of variables that have little (or sometimes completely lack of) physical meaning. On the other hand, model-based techniques, as the name implies, use a description of a system (models based on first principles or physical laws) to determine the current operating condition.

A compromise between both classes of FDI techniques is often needed when dealing with complex nonlinear systems, given the difficulty of collecting useful faulty data (a critical aspect in any data-driven FDI approach) and the expertise needed to build a reliable model of the monitored system (a key issue in a model-based FDI approach).

From a nonlinear Bayesian state estimation standpoint, this compromise between data-driven and model-based techniques may be accomplished by the use of a Particle Filter (PF) based module built upon the dynamic state model describing the time progression or evolution of the fault (Orchard & Vachtsevanos, 2009; Chen, Brown, Sconyers, Vachtsevanos, & Zhang, 2010;

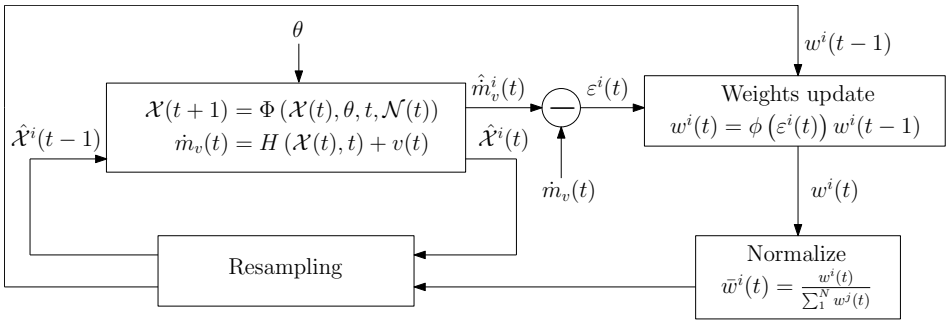

Figure 3: Block diagram of the PF algorithm for state estimation

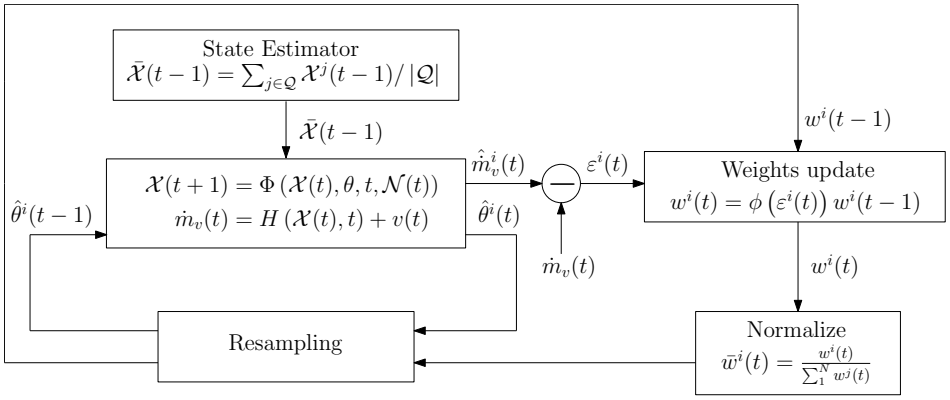

Figure 4: Block diagram of the PF algorithm for parameter estimation where $|\mathcal{Q}|$ denotes the cardinality of the set $\mathcal{Q} = \left\{ j \in 1, \ldots, N : x_{d,2}^j(t-1) = 1 \right\}$.

Orchard & Vachtsevanos, 2007). The fault progression is often nonlinear and, consequently, the model should be nonlinear as well. Thus, the diagnostic model is described by:

$$\begin{aligned} x_d(t+1) &= f_d(x_d(t), n(t)) \\ x_c(t+1) &= f_t(x_d(t), x_c(t), \omega(t)) \\ y(t) &= h_t(x_d(t), x_c(t), v(t)) \end{aligned} \tag{10}$$

where f_b, f_t, and h_t are nonlinear mappings, $x_d(t)$ is a collection of Boolean states associated with the presence of a particular operating condition in the system (normal operation, fault type #1, #2, etc.), $x_c(t)$ is a set of continuous-valued states that describe the evolution of the system given those operating conditions, $y(t)$ denotes the available measurements, $\omega(t)$ and $v(t)$ are non-Gaussian distributions that characterize the process and feature noise signals respectively. Since the noise signal $n(t)$ is a measure of uncertainty associated with Boolean states, it is advantageous to define its probability density through a random variable with bounded domain. For simplicity, $n(t)$ may be assumed to be uniform white noise (Orchard & Vachtsevanos, 2007). The PF approach using the above model allows statistical characterization of both Boolean and continuous-valued states, as new feature data (measurements) are received. As a result, at any given instant of time, this framework provides an estimate of the probability masses associated with each fault mode, as well as a pdf estimate for meaningful physical variables in the system. Once this information is available within the FDI module, it is conveniently processed to generate proper fault alarms and to report on the statistical confidence of the detection routine.

One particular advantage of the proposed particle filtering approach is the ability to characterize the evolution in time of the above mentioned nonlinear model through modification of the probability masses associated with each particle, as new data from fault indicators are received. In addition, pdf estimates for the system continuous-valued states provide the capability of performing swift transitions to failure prognosis algorithms, one of the main advantages offered by the proposed approach.

The PF based FDI module is implemented accordingly using the non-linear time growth model given in Eq. (9) to describe the expected leaked mass flow rate. The goal is for the algorithm to make an early detection of the evaporator's leakage due to an unexpected crack or a faulty connection to the evaporators pipes. Two main operating conditions are distinguished: The normal condition reflects the fact that there is no leakage while a faulty condition indicating an unexpected crack in the evaporator which causes leakage. Denote by $x_{d,1}$ and $x_{d,2}$ two Boolean states that indicate normal and faulty conditions respectively. The nonlinear model is given by:

$$\begin{aligned}\begin{bmatrix} x_{d,1}(t+1) \\ x_{d,2}(t+1) \end{bmatrix} &= f_b\left(\begin{bmatrix} x_{d,1}(t) \\ x_{d,2}(t) \end{bmatrix} + n(t)\right) \\ \dot{m}_{leak}(t) &= \theta(t) x_{d,2}(t)\sqrt{p_l(T_e(t))P_e(t)} + \omega(t) \\ \dot{m}_v(t) &= h(\dot{m}_{leak}(t), t) + v(t)\end{aligned} \tag{11}$$

where

$$f_b(x) = \begin{cases} [1 \quad 0]^T & \text{if } \left\|x - [1 \quad 0]^T\right\| \leq \left\|x - [0 \quad 1]^T\right\| \\ [0 \quad 1]^T & \text{else} \end{cases}$$

$$[x_{d,1}(t_o) \quad x_{d,2}(t_o) \quad \dot{m}_{leak}(t_o)]^T = [1 \quad 0 \quad 0]^T \tag{12}$$

In the above equations $\theta(t)$, is a time-varying model parameter that represents the crack surface (the crack constant C_r) in the evaporator that causes the leak. The one-to-one mapping $h(\cdot)$ is also referred to as fault-to-feature mapping and it is obtained using the first principles model described in Section 2. A more practical approach is to approximate the fault-to-feature mapping by a neural network that assigns the operating conditions and the leakage to the valve flow rate. In particular set $h(\dot{m}_{leak}(t), t) \cong \Psi_{NN}(\dot{m}_{leak}(t), T_e(t), T_A(t))$.

The inlet flow rate of the evaporator is substituted by $\dot{m}_v$ that denotes the TEV flow rate. It is assumed that $\dot{m}_v$ can be measured. The above system can be written in a more compact form as

$$\mathcal{X}(t+1) = \Phi(\mathcal{X}(t), \theta, t, \mathcal{N}(t)) \tag{13}$$

$$\dot{m}_v(t) = H(\mathcal{X}(t), t) + v(t) \tag{14}$$

where $\mathcal{X}^T = [x_{d,1} \quad x_{d,2} \quad \dot{m}_{leak}]^T$ and $\mathcal{V}^T = [n \quad \omega]^T$. The steps of the PF algorithm execution are described below:

1. From Eq. (13) generate N state estimates (particles) denoted by $\hat{\mathcal{X}}^i(t)$ where $i = 1, \ldots, N$. To generate the state estimates, use a zero mean Gaussian distribution for $\omega(t)$ and uniform white noise for $n(t)$.
2. From Eq. (14) calculate the liquid side flow rate estimates denoted by $\hat{\dot{m}}_v^i$, substituting the particles $\hat{\mathcal{X}}^i(t+1)$ to the mapping $H(\cdot)$.
3. Calculate the N errors $\varepsilon^i = \hat{\dot{m}}_v^i - \dot{m}_v$, and assign to each particle $\hat{\mathcal{X}}^i(t)$ a weight $w^i(t) = \phi\left(\varepsilon^i\right)$, where $\phi(\cdot)$ denotes the standard normal distribution.
4. Normalize the weights $w^i(t)$. The normalized weights $\bar{w}^i(t)$ represent the discrete probability masses of each state estimate.
5. Calculate the final state estimate $\widetilde{\mathcal{X}}(t)$ using the weighted sum of all the states $\hat{\mathcal{X}}^i(t)$.

An important part of the PF algorithm is the resampling procedure. Resampling is an action that takes place to counteract the degeneracy of the particles caused by estimates that have very low weights. A block diagram of the PF algorithm is given in Figure 3. An obvious shortcoming of the above procedure is that the crack coefficient C_r is unknown in a real life application. To this extent we augment to the standard FDI algorithm a parameter estimator module utilizing also PF with the objective to identify on-line the time-varying parameter $\theta(t)$. The parameter estimator is executed in parallel with the state estimator. The execution steps of the PF algorithm for parameter estimation are described below:

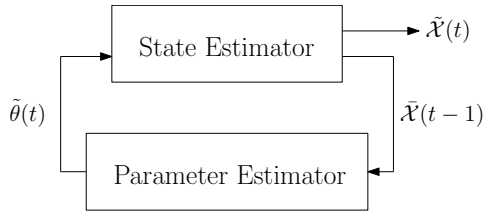

Figure 5: Block diagram of the complete FDI algorithm that utilizes a dual PF for state and parameter estimation.

1. For each faulty particle ($x_{d,2}^i(t) = 1$) calculate the mean state $\bar{\mathcal{X}}(t)$. If there are not any faulty particles exit the parameter estimation module.
2. Using $\bar{\mathcal{X}}(t)$ from Eq. (13) generate N_θ parameter estimates (particles) denoted by $\hat{\theta}^i(t)$ where $i = 1, \ldots, N_\theta$.
3. From Eq. (14) calculate the liquid side flow rate estimates denoted by $\hat{\dot{m}}_v^i$, substituting the particles $\bar{\mathcal{X}}^i(t+1)$ to the mapping $H(\cdot)$.
4. Calculate the N errors $\varepsilon^i = \hat{\dot{m}}_v^i - \dot{m}_v$, and assign to each particle $\hat{\theta}^i(t)$ a weight $w^i(t) = \phi\left(\varepsilon^i\right)$, where $\phi(\cdot)$ denotes the standard normal distribution.
5. Normalize the weights $w^i(t)$. The normalized weights $\bar{w}^i(t)$ represent the discrete probability masses of each state estimate.
6. Calculate the final state estimate $\widetilde{\theta}(t)$ using the weighted sum of all the states $\hat{\theta}^i(t)$.

The resampling module takes place is an identical way as for the state estimator. A block diagram of the PF algorithm for parameter estimation is given in Figure 4. The interconnection of the two PF modules for both state and parameter estimation is given in Figure 5.

5. PROGNOSIS

Prognosis can be essentially understood as the generation of long-term predictions describing the evolution in time of a particular signal of interest or fault indicator. The goal of the prognostic algorithm is to use the evolution of the fault indicator in order to estimate the RUL of a failing component. Since prognosis intends to project the current condition of the indicator, it necessarily entails large-grain uncertainty. This paper adopts a prognosis scheme based on recursive Bayesian estimation techniques, combining the information from fault growth models and on-line data from sensors monitoring the plant.

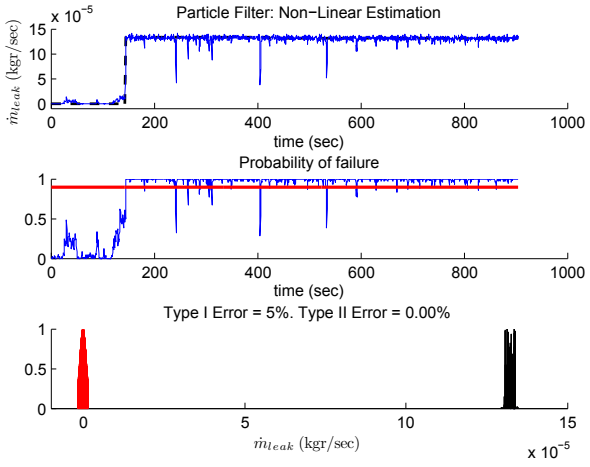

Figure 6: PF based FDI module

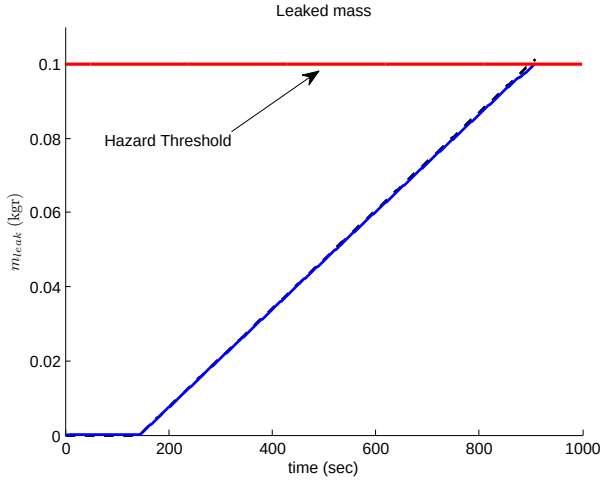

Figure 7: This figure illustrates the actual (dashed line) and the estimated (solid line) value of the leaked mass.

The prognosis algorithm is activated when a fault has been declared by the FDI module. Prognosis is a problem that goes beyond the scope of filtering applications, since it involves future time horizons. The main idea of the prognostic algorithm is to project the continuous state particle population in time, using the fault growth model, in order to estimate the time-to-failure (TTF) of each particle. Considering the nonlinear model given in Eq. (11) and using the notation of the diagnostic model introduced in Eq. (10), the progression in time of the continuous state can be written us:

$$x_c(t+1) = \psi\big(x_c(t), t\big) \tag{15}$$

The above equation represents the nonlinear mapping $f_t(\cdot)$, initially introduced in Eq. (10). From this mapping we have excluded the dependence of the noise $\omega(t)$ and the dependence of the boolean state $x_d(t)$, since in the prognostic mode a fault has already been detected. The inclusion of the time variable in the definition of the nonlinear mapping $\psi(\cdot)$ allows the investigation of time varying fault growth models. The execution of the prognostic algorithm at each time instant includes the following steps:

1. At each time instant, receive from the fault detection module N particles of the continuous state denoted by $\hat{x}_c^i(t)$, where $i = 1, \ldots, N$. For each particle, using the fault growth model, iterate p^i steps in time, with $p^i \in \mathbb{N}$, such that the p^i-step ahead predictions given by:

$$\hat{x}_c^i(t+p^i) = \psi\Big(\hat{x}_c^i(t+p^i-1), (t+p^i-1)\Big)$$

   are such that $X_{hazard}^{low} \leq \hat{x}_c^i(t+p^i) \leq X_{hazard}^{high}$, where X_{hazard}^{low}, X_{hazard}^{high} denote the upper and lower bounds of a hazard zone that designate the limits of a critical failure. The initial estimates $\hat{x}_c^i$ are taken directly by the PF detection algorithm described in the previous section.

2. Using the RUL estimates (p^i) and the normalized weights of the detection algorithm ($\bar{w}^i(t)$), the pdf and the weighted estimate of the RUL, denoted as $\hat{t}_{RUL}$, can be obtained for each time step.

In many practical applications, the error that can be generated by considering the particle weights invariant for future time instants is negligible with respect to other sources, such as model inaccuracies or wrong assumptions about process/measurement noise parameters. Thus, from this standpoint, Eq. (15) is considered sufficient to extend the fault estimate trajectories, while the current particle weights are propagated in time without changes. The computational burden of this method is considerably reduced and, as it will be shown in simulation results, it can give a satisfactory view about how the system behaves in time for most practical applications.

The proposed fault diagnosis framework allows the use of the pdf estimates of the system continuous valued states (computed at the moment of fault detection) as initial conditions in the failure prognostic routine, giving excellent insight into the inherent uncertainty in the prediction problem. As a result, a swift transition between the two modules (fault diagnosis and failure prognosis) may be performed, and moreover, reliable prognosis can be achieved within a few cycles of operation after the fault is declared. This characteristic is, in fact, one of the main advantages offered by this particle-filter based framework.

6. SIMULATION RESULTS

The performance of the proposed FDI and prognostic algorithms was tested via numerical simulations. The evaporator dynamics are described by Eqs. (1)-(7). Regarding the inlet flow rates we set:

$$\dot{m}_{in} = \dot{m}_v - \dot{m}_{leak} \text{ and } \dot{m}_{out} = \dot{m}_c$$

where $\dot{m}_v$ and $\dot{m}_c$ are the flow rates of the TEV and compressor, respectively. The leakage fault is seeded according to Eq. (9). The systems parameters are summarized in Table 1. The number of particles used for the two estimators (state and parameter) are $N = 100$ and $N_\theta = 150$. The crack constant is given by:

$$C_r(t) = 5 \cdot 10^{-9} step(t - 144) \tag{16}$$

Using the above representation we simulate the occurrence of an and abrupt and unexpected crack that causes

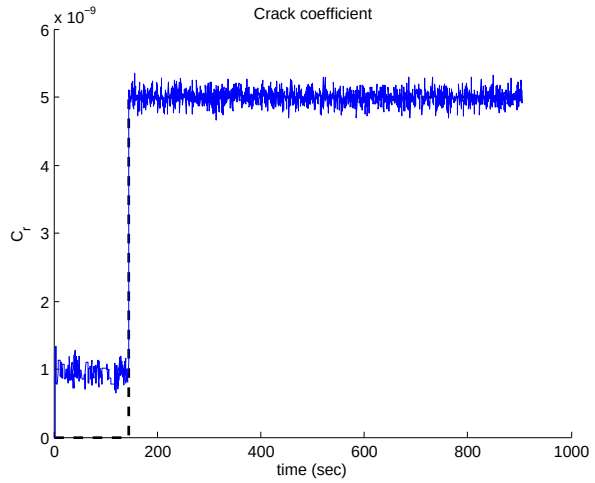

Figure 8: This figure illustrates the actual (dashed line) and the estimated (solid line) value of the crack coefficient.

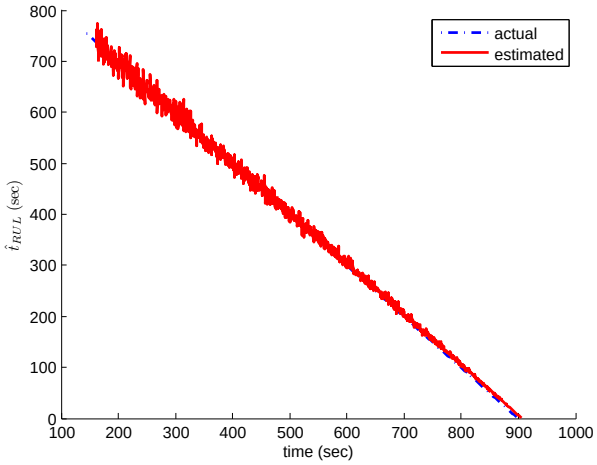

Figure 9: This figure illustrates the actual (dashed dotted line) and the estimated (solid line) value of RUL.

Table 1: Simulator parameters

$\bar{\gamma}$	0.8474	A_w	$6.6361 \cdot 10^{-5}\, m^2$
A_t	$3.14 \cdot 10^{-2}\, m^2$	$U_w A_w$	$40.9962\, W/K$
U_w	$592.9817\, W/K m^2$	$\dot{m}_a$	$0.765\, kgr/sec$
D_t	$0.02\, m$	c_a	$10^3\, J/kgr \cdot K$
V_e	$0.0057\, m^3$	ρ_a	$1.1996\, kgr/m^3$
c_w	$1.9552 \cdot 10^3 J/kgr \cdot K$	A_a	$0.1518\, m^2$
ρ_w	$7.8491 \cdot 10^3\, kgr/m^3$	x	0

the nonlinear leakage growth model given in Eq. (9). Signal noise has been added to the available measurements. The saturated states are calculated based on the tables of $R134a$ refrigerant. The operating conditions are $\dot{m}_v = \dot{m}_c = 0.0108\, kgr/sec$ and $T_A = 26\, C^o$. Besides detecting the faulty condition, it is desired to obtain some measure of the statistical confidence of the alarm signal. For this reason, two outputs will be extracted from the FDI module. The first output is the expectation of the Boolean state $x_{d,2}(t)$, which constitutes an estimate of the probability of fault. The second output is the statistical confidence needed to declare the fault via hypothesis testing (H_0: 'the evaporator is not leaking' vs H_1: 'The evaporator is leaking'). The latter output needs another pdf to be considered as the baseline. In this case, a normal distribution $N(0, \sigma)$ is used to define this baseline data. This indicator is essentially equivalent to an estimate of type II error. Customer specifications are translated into acceptable margins for the type I and II errors in the detection routine.

The algorithm itself will indicate when the type II error (false negatives) has decreased to the desired level. Figure 6 shows two indicators that are simultaneously computed. The first indicator, depicted as a function of time, shows the probability of a determined failure mode, and it is based on the estimate of the Boolean state $x_{d,2}$. FDI alarms may be triggered whenever this indicator reaches a pre-determined threshold (in this case the threshold value is 0.9). If more information is needed, the type II detection error (second and third indicators, respectively) may be considered.

Figure 7 illustrates the actual and estimated leaked mass. Figure 8 illustrates the estimated crack coefficient. A small bias is evident in the crack coefficient estimate in the healthy condition. However, this bias has a very small value and a low probability of fault. Finally Figure 9 illustrates the actual RUL compared to $\hat{t}_{RUL}$ that is estimated by the prognosis module. The results indicate that the enhanced FDI and prognostic algorithms provide very accurate estimates of the fault progression, the crack coefficient and the RUL estimate.

7. CONCLUSIONS

This paper is introducing an architecture for the development, implementation, testing and assessment of a particle-filtering-based framework for FDI and prognosis. The proposed framework for FDI has been successful and very efficient in pinpointing abnormal conditions in very complex and nonlinear processes, such as the detection of leakage in a two-phase evaporator of an ECS. The FDI algorithm is enhanced with an adaptive mod-

ule that provides estimates of the fault nonlinear model parameters. Regarding prognosis, it was shown that that the proposed approach is suitable for online implementation, providing acceptable results in terms of precision and accuracy. A successful case study has been presented, offering insights about how model inaccuracies and/or customer specifications (hazard zone or prediction window definitions) may affect the algorithm performance.

REFERENCES

Braun, J. (2003). Automated Fault Detection and Diagnostics for Vapor Compression Cooling Equipment. *Transaction of the ASME*, *125*, 266-274.

Breuker, M., & Braun, J. (1998). Common faults and their impacts for rooftop air conditioners. *International Journal of HVAC&R Reserach*, *4*, 303-318.

Chen, C., Brown, D., Sconyers, C., Vachtsevanos, G., & Zhang, B. (2010). A .NET framework for an integrated fault diagnosis and failure prognosis architecture. In *IEEE AUTOTESTCON*.

Chen, C., Vachtsevanos, G., & Orchard, M. (2010). Machine remaining useful life prediction based on adaptive neuro-fuzzy and high-order particle filtering. In *Annual Conference of the Prognostics and Health Management Society.*

Chen, C., Zhang, B., & Vachtsevanos, G. (n.d.). *Prediction of machine health condition using neuro-fuzzy and Bayesian algorithms.* (To be published in IEEE Transactions on Instrumentation and Measurement)

Cheng, T., He, X.-D., & Asada, H. (2004). Nonlinear observer design for two-phase flow heat exchangers of air conditioning systems. In *American Control Conference, 2004. Proceedings of the 2004* (Vol. 2, p. 1534 - 1539 vol.2).

Comstock, M., Braun, J., & Groll, E. (2002). A survey of common faults for chillers. *ASHRAE Transactions*, *108*, 819-825.

Grald, E. W., & MacArthur, J. (1992). A moving-boundary formulation for modeling time-dependent two-phase flows. *International Journal of Heat and Fluid Flow*, *13*(3), 266 - 272.

He, X. (1996). *Dynamic Modeling and Multivariable Control of Vapor Compression Cycles in Air Conditioning Systems*. Unpublished doctoral dissertation, Massachusetts Institute of Technology.

He, X.-D., & Asada, H. (2003). A new feedback linearization approach to advanced control of multi-unit HVAC systems. In *American Control Conference, 2003. Proceedings of the 2003* (Vol. 3, p. 2311 - 2316 vol.3).

Li, H., & Braun, J. (2003). An Improved Method for Fault Detection and Diagnosis Applied to Packaged Air Conditioners. *American Society of Heating, Refrigerating and Air Conditioning Engineers*, *109*, 683-692.

Merritt, H. (1967). *Hydraulic Control Systems*. John Wiley & Sons.

Navarro-Esbri, J., Torrella, E., & Cabello, R. (2006). A vapour compression chiller fault detection technique based on adaptative algorithms. Application to on-line refrigerant leakage detection. *International Journal of Refrigeration*, *29*, 716-723.

Orchard, M., & Vachtsevanos, G. (2007). A particle filtering-based framework for real-time fault diagnosis and failure prognosis in a turbine engine. In *Control Automation, 2007. MED '07. Mediterranean Conference on* (p. 1 -6).

Orchard, M., & Vachtsevanos, G. (2009). A particle-filtering approach for on-line fault diagnosis and failure prognosis. *Transactions of the Institute of Measurment and Control*, *31*, 221-246.

Rasmussen, B. (2005). *Dynamic Modeling and Advanced Control of Air Conditioning and Refrigeration Systems*. Unpublished doctoral dissertation, University of Illinois.

Rossi, T., & Braun, J. (1997). A statistical, rule-based fault detection and diagnostic method for vapor compression air conditioners. *International Journal of HVAC&R Reserach*, *3*, 19-37.

Stylianou, M., & Nikanpour, D. (1996). Performance monitoring, fault detection, and diagnosis of reciprocating chillers. *ASHRAE Transactions*, *102*, 615-627.

Wedekind, G., Bhatt, B., & Beck, B. (1978). A System Mean void Fraction Model For Predicting Various Transient Phenomena Associated with Two-Phase Evaporating and Condensing Flows. *International journal of Multiphase Flow*, *4*, 97-114.

Ioannis A. Raptis was born in Athens, Greece in 1979. He received his Dipl-Ing. in Electrical and Computer Engineering from the Aristotle University of Thessaloniki, Greece and his Master of Science in Electrical and Computer Engineering from the Ohio State University in 2003 and 2006, respectively. From 2005 until 2006 he conducted research at the Locomotion and Biomechanics Laboratory of the Ohio State University. In 2006 he joined the Unmanned Systems Laboratory at the University of South Florida. In 2010 he received his Ph.D. degree in the department of Electrical Engineering at the University of South Florida. In 2010 he joined the Intelligent Control Systems Laboratory of the Georgia Institute of Technology. His research interests include nonlinear systems control theory, nonlinear control of electromechanical/robotic systems and rotorcraft/aircraft system identification and control.

George J. Vachtsevanos is a Professor Emeritus of Electrical and Computer Engineering at the Georgia Institute of Technology. He was awarded a B.E.E. degree from the City College of New York in 1962, a M.E.E. degree from New York University in 1963 and the Ph.D. degree in Electrical Engineering from the City University of New York in 1970. He directs the Intelligent Control Systems laboratory at Georgia Tech where faculty and students are conducting research in intelligent control, neurotechnology and cardiotechnology, fault diagnosis and prognosis of large-scale dynamical systems and control technologies for Unmanned Aerial Vehicles. Dr. Vachtsevanos was awarded the IEEE Control Systems Magazine Outstanding Paper Award for the years 2002-2003 (with L. Wills and B. Heck). He was also awarded the 2002-2003 Georgia Tech School of Electrical and Computer Engineering Distinguished Professor Award and the 2003-2004 Georgia Institute of Technology Outstanding Interdisciplinary Activities Award.